

NUMERICAL APPROXIMATION OF ASYMPTOTICALLY DISAPPEARING SOLUTIONS OF MAXWELL'S EQUATIONS*

J. H. ADLER[†], V. PETKOV[‡], AND L. T. ZIKATANOV[§]

Abstract. This work is on the numerical approximation of incoming solutions to Maxwell's equations with dissipative boundary conditions, whose energy decays exponentially with time. Such solutions are called asymptotically disappearing (ADS) and they play an important role in inverse back-scattering problems. The existence of ADS is a difficult mathematical problem. For the exterior of a sphere, such solutions have been constructed analytically by Colombini, Petkov, and Rauch [*Proc. Amer. Math. Soc.*, 139 (2011), pp. 2163–2173] by specifying appropriate initial conditions. However, for general domains of practical interest (such as Lipschitz polyhedra), the existence of such solutions is not evident. This paper considers a finite-element approximation of Maxwell's equations in the exterior of a polyhedron, whose boundary approximates the sphere. Standard Nédélec–Raviart–Thomas elements are used with a Crank–Nicolson scheme to approximate the electric and magnetic fields. Discrete initial conditions interpolating the ones chosen by Colombini, Petkov, and Rauch are modified so that they are (weakly) divergence-free. We prove that with such initial conditions, the approximation to the electric field is weakly divergence-free for all time. Finally, we show numerically that the finite-element approximations of the ADS also approximates this exponential decay (quadratically) with time when the mesh size and the time step become small.

Key words. Maxwell's equations, finite-element method, dissipative boundary conditions, asymptotically disappearing solutions

AMS subject classifications. 65M60, 35Q61, 65Z05

DOI. 10.1137/120879385

1. Introduction. This paper studies the numerical approximation of incoming solutions to Maxwell's equations in terms of the electric field, $\mathbf{E}(t, \mathbf{x})$, and the magnetic field, $\mathbf{B}(t, \mathbf{x})$,

$$\begin{aligned} \varepsilon \mathbf{E}_t - \operatorname{curl} \mu^{-1} \mathbf{B} &= -\mathbf{j}, & \mathbf{B}_t + \operatorname{curl} \mathbf{E} &= 0, \\ \operatorname{div} \varepsilon \mathbf{E} &= 0, & \operatorname{div} \mathbf{B} &= 0, \end{aligned}$$

in the exterior of a spherical obstacle, with dissipative boundary condition on the sphere (see (1.1)). Here, ε is the permittivity of the medium, μ is the permeability, and $\operatorname{div} \mathbf{j} = 0$, where \mathbf{j} is the known current density of the system. We approximate numerical solutions, whose total energy decays exponentially with time. Such solutions are called *asymptotically disappearing* (ADS) and this phenomenon is of interest for inverse back-scattering problems, since the leading term of the back-scattering matrix becomes negligible. Details and construction of such solutions for the exterior of the unit sphere are found in the recent work by Colombini, Petkov, and Rauch [10]. The dissipative boundary conditions of interest are

$$(1.1) \quad (1 + \gamma) \mathbf{E}_{\tan} = -\mathbf{n} \wedge \mu^{-1} \mathbf{B}_{\tan} \quad \text{on the boundary of the obstacle.}$$

*Received by the editors June 1, 2012; accepted for publication (in revised form) June 25, 2013; published electronically October 28, 2013. This work was supported in part by U.S. Department of Energy grant DE-FG02-11ER26062/DE-SC0006903 and subcontract LLNL-B595949.

<http://www.siam.org/journals/sisc/35-5/87938.html>

[†]Department of Mathematics, Tufts University, Medford, MA 02155 (james.adler@tufts.edu).

[‡]Institut de Mathématiques de Bordeaux, 351 Cours de la Libération, 33405 Talence, France (petkov@math.u-bordeaux1.fr).

[§]Department of Mathematics, Penn State University, University Park, PA 16802 (ludmil@psu.edu). This author's work was supported in part by National Science Foundation grants DMS-0810982 and DMS-1217142.

Here, \mathbf{n} is the outward unit normal to the boundary and γ is a parameter satisfying $\gamma > 0$.

For a spherical obstacle, a case on which we focus here, the boundary is $|\mathbf{x}| = 1$. In [10], it is shown that for any value of the parameter $\gamma > 0$ determining the dissipative boundary condition, there exist initial conditions such that the boundary value problem for Maxwell’s equations has a solution, which decays exponentially in time as $\mathcal{O}(e^{rt})$, with $r < 0$. It is also interesting to note that in space such solutions also decay asymptotically at infinity, i.e., they behave as $\mathcal{O}(e^{r|\mathbf{x}|})$ (see [20]). Moreover, for dissipative boundary conditions, (1.1), if $\gamma > 0$, there are no disappearing solutions, $u(T, x)$, that vanish for all $t \geq T > 0$ in the exterior of the sphere (see [12]).

The focus of this work is on the finite-element approximation of the ADS in the exterior of a polyhedron that approximates the sphere. This is a first step toward developing numerical techniques, which later can be used to construct approximations to ADS for more complicated obstacles and also for other symmetric hyperbolic systems with dissipative boundary conditions. Such a general study is feasible due to a recent result of Colombini, Petkov, and Rauch [11] for hyperbolic systems whose solutions are described by a contraction semigroup $V(t) = e^{Gt}$, $t > 0$. More precisely, it was shown in [11] that if certain coercivity estimates are satisfied, then the spectrum of the generator, G , in the left half plane, $\text{Re}(z) < 0$, is formed only by discrete eigenvalues with finite multiplicities. Every such eigenvalue, $\lambda : \text{Re}(\lambda) < 0$, yields an ADS solution, $u(t, x) = e^{\lambda t} f(x)$, with $Gf = \lambda f$. We notice that in [10] only real eigenvalues of the generator G have been constructed. The question of the existence of complex eigenvalues is open and numerical results can shed light on the open question of existence of complex eigenvalues.

On the other hand, the *existence* and the *location* of eigenvalues of G for less regular obstacles is a difficult and interesting mathematical problem (from both theoretical and numerical points of view), although it falls beyond the scope of the work reported here.

For the finite-element spaces that we use, their properties and implementation in the numerical models based on Maxwell’s system are more or less known. Classical references on the piecewise polynomial spaces relevant in such approximations are the papers by Raviart and Thomas [21] (for two spatial dimensions), Nédélec [16, 17], and Bossavit [7]. The method that is used here is an application of the techniques developed by Brezzi [8] (see also Brezzi and Fortin [9]). Many results and references on Maxwell’s system and its numerical approximation are found in Hiptmair’s work [13] and in a monograph by Monk [15]. In most of these works, the emphasis is on systems with perfect conductor boundary conditions. The important difference between our work and the previous ones is that here we apply the methods to a problem with dissipative boundary conditions, where the electric field, \mathbf{E} , and the magnetic field, \mathbf{B} , are paired together. A related discussion on the role of the boundary conditions in the numerical solution of systems of PDEs is given in a recent paper by Arnold, Falk, and Gopalakrishnan [2].

We consider the finite-element problem associated with Maxwell’s equations in a finite domain between two spheres, $\Omega = \{\mathbf{x} \mid 1 < |\mathbf{x}| < R\}$, for a fixed, large enough R . The discretization of Maxwell’s equations that keeps the coupling between the electric and the magnetic field intact, and can be derived via the modern techniques in finite-element exterior calculus, is described in Arnold, Falk, Gopalakrishnan, and Winther [1, 3]. We obtain a computational domain (denoted again with Ω), which is *polyhedron* and which *approximates* the exterior of the annular domain $\{\mathbf{x} \mid 1 < |\mathbf{x}| < R\}$. Note that the ADS constructed in [10] for the exterior of the sphere do

not need to satisfy the dissipative boundary condition on the polyhedron. However, we show numerically that the finite-element solution with initial conditions approximating those in [10] yields good approximation of the ADS constructed analytically, when the mesh size becomes small and the polyhedron gets closer to the sphere.

This paper is organized as follows. In section 2, we introduce some notation and state the strong form of the boundary value problem for Maxwell's equations that we consider. Section 3 describes the variational (weak) formulation and discusses the energy decay of the corresponding system. Next, we discuss the discretization of this variational form and how we can guarantee a good approximation of the ADS in section 4. In section 5, we describe the matrix representation of the semidiscrete system and the properties of the Crank–Nicolson scheme that we use for time stepping. Numerical results for the sphere are shown in section 6. Finally, concluding remarks and discussions on constructing initial conditions as well as a choice of parameters for more complicated obstacles are presented in section 7.

2. Notation and preliminaries. First, some standard notation is introduced, which is needed in the following sections. The Euclidean scalar product between two vectors in \mathbb{R}^d is denoted by $\langle \mathbf{a}, \mathbf{b} \rangle$ and the corresponding norm is $|\mathbf{a}|^2 = \langle \mathbf{a}, \mathbf{a} \rangle$. The standard $L^2(\Omega)$ scalar product and norm are denoted by (\cdot, \cdot) and $\|\cdot\|$, respectively.

2.1. Maxwell's system. The system of PDEs of interest is Maxwell's system with a dissipative boundary condition (impedance boundary condition). Let \mathcal{O} be a bounded, connected (could be convex) domain, $\mathcal{O} \subset \mathbb{R}^3$. As stated in the introduction, we consider Maxwell's equations in the exterior of $\overline{\mathcal{O}}$, that is, in $\Omega = \mathbb{R}^3 \setminus \overline{\mathcal{O}}$, which is as follows:

$$(2.1) \quad \varepsilon \mathbf{E}_t - \operatorname{curl} \mu^{-1} \mathbf{B} = -\mathbf{j},$$

$$(2.2) \quad \mathbf{B}_t + \operatorname{curl} \mathbf{E} = 0,$$

$$(2.3) \quad \operatorname{div} \varepsilon \mathbf{E} = 0,$$

$$(2.4) \quad \operatorname{div} \mathbf{B} = 0.$$

For the rest of the paper, we assume that the permittivity, ε , and the permeability, μ , are equal to 1. Future work will involve investigating numerical methods when these parameters are allowed to vary with the domain. We also assume that Ω is bounded, which means $\Omega = \mathcal{S} \setminus \overline{\mathcal{O}}$, where \mathcal{S} is a ball in \mathbb{R}^3 with sufficiently large radius. While in general this could be a restriction, in this case it is not, since the solutions that are approximated decay exponentially when $|\mathbf{x}| \rightarrow \infty$.

2.2. Dissipative boundary conditions. The boundary conditions that are of interest are also known as impedance boundary conditions. To state such type of boundary condition, we first define

$$\Gamma_i = \partial\Omega \cap \partial\mathcal{O}, \quad \Gamma_o = \partial\Omega \setminus \Gamma_i,$$

where Γ_i represents the boundary of the inner obstacle and Γ_o the outer boundary (i.e., the boundary of \mathcal{S}). The orthogonal projection, Q_{\tan} , on the component of a vector field tangential to Γ_i is also needed, which for any $\mathbf{x} \in \Gamma_i$ and a vector field $\mathbf{F}(\mathbf{x}) \in \mathbb{R}^3$ is defined as the tangential component of $\mathbf{F}(\mathbf{x})$, namely,

$$\mathbf{F}_{\tan} = Q_{\tan} \mathbf{F} = \mathbf{F} - \langle \mathbf{F}, \mathbf{n} \rangle \mathbf{n} = -\mathbf{n} \wedge (\mathbf{n} \wedge \mathbf{F}),$$

where \mathbf{n} is the normal vector to the surface Γ_i . We denote by \mathbf{n} the normal pointing away from the domain (i.e., pointing into \mathcal{O}). We note that all the quantities above

depend on $\mathbf{x} \in \Gamma_i$. The boundary condition of interest is the one in (1.1) and it is recalled here:

$$(1 + \gamma)\mathbf{E}_{\text{tan}} = -\mathbf{n} \wedge \mathbf{B}_{\text{tan}} \quad \text{or equivalently} \quad (1 + \gamma)\mathbf{E}_{\text{tan}} = -\mathbf{n} \wedge \mathbf{B}.$$

As pointed out above, $\gamma > 0$ is a constant, i.e., $\gamma \in \mathbb{R}$. However, the same methods can be applied for $\gamma(x) > 0$ as a function on the boundary of the domain.

Remark 2.1. Note that for a perfectly conducting obstacle, the tangential component of \mathbf{E} vanishes on the boundary, namely,

$$\mathbf{E} \wedge \mathbf{n} = \mathbf{0}, \quad \mathbf{x} \in \partial\Omega.$$

However, again, this paper considers the case of an impedance condition, where the obstacle is not a perfect conductor. This is closer to real-world applications, where dissipative boundary conditions occur frequently.

3. Function spaces and variational formulation.

3.1. Function spaces. To approximate the differential problem (2.1)–(2.4) with the boundary conditions given in (1.1), the function spaces for the problem at hand need to be identified. Given a Lipschitz domain, Ω , and a differential operator, \mathcal{D} , a standard notation for the following spaces is used:

$$H(\mathcal{D}) = \{\mathbf{v} \in (L^2(\Omega))^{d_1}, \mathcal{D}\mathbf{v} \in (L^2(\Omega))^{d_2}\}$$

with the associated graph norm,

$$\|\mathbf{u}\|_{\mathcal{D};\Omega}^2 = \|\mathbf{u}\|^2 + \|\mathcal{D}\mathbf{u}\|^2,$$

where d_1 is the dimension of the problem (three for this paper) and d_2 depends on the operator. By taking $\mathcal{D} = \text{div}$ ($d_2 = 1$) or $\mathcal{D} = \text{curl}$ ($d_2 = 3$), the Sobolev spaces $H(\text{div})$ and $H(\text{curl})$ are obtained. Also, notice that

$$H^1(\Omega) = H(\text{grad}), \quad L^2(\Omega) = H(\text{id}), \quad d_2 = 3.$$

For example, $H(\text{curl})$ is the space of $L^2(\Omega)$ vector-valued functions, whose curl is also in $L^2(\Omega)$, and similarly for $H(\text{grad})$ and $H(\text{div})$.

The following three spaces are needed (the first one for scalar functions and the second and third for vector-valued functions):

$$\begin{aligned} H_0(\text{grad}) &= H_0^1(\Omega) = \{v \in H^1(\Omega) \quad \text{such that} \quad v|_{\partial\Omega} = 0\}, \\ \tilde{H}_{\text{imp}}(\text{curl}) &= \{\mathbf{v} \in H(\text{curl}) \quad \text{such that} \quad \mathbf{v} \wedge \mathbf{n}|_{\Gamma_o} = 0\}, \\ H_{\text{imp}}(\text{div}) &= \{\mathbf{v} \in H(\text{div}) \quad \text{such that} \quad \langle \mathbf{v}, \mathbf{n} \rangle|_{\Gamma_o} = 0\}. \end{aligned}$$

Note that the tangential component of the electric field, \mathbf{E} , on $\Gamma_o = \partial\Omega \setminus \Gamma_i$, is set to zero for the elements of $\tilde{H}_{\text{imp}}(\text{curl})$. From this and the fact that $\mathbf{B}_t = -\text{curl} \mathbf{E}$, it follows that the normal component of the magnetic field \mathbf{B} is also zero on this outer boundary, which is the boundary condition incorporated in $H_{\text{imp}}(\text{div})$.

Another issue to address is related to the fact that the boundary of the computational domain consists of two connected components Γ_i and Γ_o , which is an artifact of how we treat the far field. Even though there are methods, such as perfectly matched layer and absorbing boundary conditions, that treat the far field more accurately, the solutions presented here decay rapidly in space and, therefore, we can simply add an outer boundary with homogeneous Dirichlet boundary conditions. If the initial conditions is a harmonic form for \mathbf{E} and $\mathbf{B}_0 = 0$, then, as is easily computed, the solution

does not change in time. If we did not have the outer boundary, then such phenomena will not happen. From this, it can be concluded that if a harmonic form is part of the initial condition, then this part is going to be unchanged when propagated in time. However, since the goal is to show that the energy of the system dissipates over time (for any initial condition that does not have the harmonic form as a component), we consider only initial conditions that are orthogonal to the space of harmonic forms. To resolve the ambiguity, we consider electric fields in a subspace of $\tilde{H}_{\text{imp}}(\text{curl})$, which is orthogonal to the one-dimensional space of harmonic forms. Let \mathfrak{h} be the unique solution to the Laplace equation:

$$(3.1) \quad -\Delta \mathfrak{h} = 0, \quad \mathfrak{h} = 1 \quad \text{on } \Gamma_i, \quad \text{and} \quad \mathfrak{h} = 0 \quad \text{on } \Gamma_o.$$

Then, define $H_{\text{imp}}(\text{curl})$ as the space of functions orthogonal to $\text{grad } \mathfrak{h}$:

$$(3.2) \quad H_{\text{imp}}(\text{curl}) = \{\mathbf{v} \in \tilde{H}_{\text{imp}}(\text{curl}) \text{ such that } (\mathbf{v}, \text{grad } \mathfrak{h}) = 0\}.$$

Finally, for the time-dependent problem considered here, the relevant function spaces are

$$\begin{aligned} H_0(\text{grad}; t) &= \{v(t, \cdot) \in H_0^1(\Omega) \text{ for all } t \geq 0\}, \\ H_{\text{imp}}(\text{curl}; t) &= \{\mathbf{v}(t, \cdot) \in H_{\text{imp}}(\text{curl}) \text{ for all } t \geq 0\}, \\ H_{\text{imp}}(\text{div}; t) &= \{\mathbf{v}(t, \cdot) \in H_{\text{imp}}(\text{div}) \text{ for all } t \geq 0\}. \end{aligned}$$

In another words, if $H(\mathcal{D})$ denotes any of the Hilbert spaces $H_0(\text{grad})$, $H_{\text{imp}}(\text{curl})$, or $H_{\text{imp}}(\text{div})$, then $H(\mathcal{D}; t)$ is the space of functions, which for each $t \in [0, \infty)$ takes on values in $H(\mathcal{D})$. We assume that the elements of any of the spaces $H_0(\text{grad}; t)$, (resp., $H_{\text{imp}}(\text{curl}; t)$ or $H_{\text{imp}}(\text{div}; t)$) are differentiable with respect to t as many times as needed. We refer to McLean [14] and also Monk [15] for properties of the above spaces and related density results.

3.2. Variational formulation. Next, we derive a weak form which was shown to us by Arnold [4]. We introduce $p \in H_0(\text{grad}; t)$ such that

$$(3.3) \quad (p_t, q) = (\mathbf{E}, \text{grad } q) \quad \text{for all } q \in H_0(\text{grad}), \quad p(0, \mathbf{x}) = 0.$$

This is an auxiliary variable associated with the constraint that \mathbf{E} is divergence-free. If the initial condition for \mathbf{E} is divergence-free, then as shown below, p is zero for all times. However, if the initial guess is not divergence-free, then p does not have to be zero.

First, multiply (2.2) and (2.1) by test functions $\mathbf{C} \in H_{\text{imp}}(\text{div})$ and $\mathbf{F} \in H_{\text{imp}}(\text{curl})$, respectively. Next, integrate by parts and use boundary conditions (1.1) and the identities

$$\langle \mathbf{n} \wedge \mathbf{B}, \mathbf{F} \rangle = \langle (\mathbf{n} \wedge \mathbf{B}_{\text{tan}}), \mathbf{F}_{\text{tan}} \rangle, \quad \langle \mathbf{E}_{\text{tan}}, \mathbf{F}_{\text{tan}} \rangle = \langle \mathbf{n} \wedge \mathbf{E}, \mathbf{n} \wedge \mathbf{F} \rangle$$

to obtain for all $\mathbf{C} \in H_{\text{imp}}(\text{div})$ and for all $\mathbf{F} \in H_{\text{imp}}(\text{curl})$,

$$(3.4) \quad \begin{aligned} (\mathbf{B}_t, \mathbf{C}) + (\text{curl } \mathbf{E}, \mathbf{C}) &= 0, \\ (\mathbf{E}_t, \mathbf{F}) + (\nabla p, \mathbf{F}) - (\mathbf{B}, \text{curl } \mathbf{F}) + (1 + \gamma) \int_{\Gamma_i} \langle \mathbf{n} \wedge \mathbf{E}, \mathbf{n} \wedge \mathbf{F} \rangle d\gamma &= -(\mathbf{j}, \mathbf{F}). \end{aligned}$$

Finally, we get the following variational problem.

Find $(\mathbf{E}, \mathbf{B}, p) \in H_{\text{imp}}(\text{curl}; t) \times H_{\text{imp}}(\text{div}; t) \times H_0(\text{grad}; t)$, such that for all $(\mathbf{F}, \mathbf{C}, q) \in H_{\text{imp}}(\text{curl}) \times H_{\text{imp}}(\text{div}) \times H_0^1(\Omega)$ and for all $t > 0$,

$$(3.5) \quad (\mathbf{E}_t, \mathbf{F}) = -(\text{grad } p, \mathbf{F}) + (\mathbf{B}, \text{curl } \mathbf{F}) - (1 + \gamma) \int_{\Gamma_i} \langle \mathbf{E}_{\text{tan}}, \mathbf{F}_{\text{tan}} \rangle - (\mathbf{j}, \mathbf{F}),$$

$$(3.6) \quad (\mathbf{B}_t, \mathbf{C}) = -(\text{curl } \mathbf{E}, \mathbf{C}),$$

$$(3.7) \quad (p_t, q) = (\mathbf{E}, \text{grad } q).$$

At $t = 0$, the following initial conditions are needed:

$$(3.8) \quad \mathbf{E}(0, \mathbf{x}) = \mathbf{E}_0(\mathbf{x}), \quad \mathbf{B}(0, \mathbf{x}) = \mathbf{B}_0(\mathbf{x}), \quad p(0, \mathbf{x}) = 0.$$

Here, $\mathbf{E}_0 \in H_{\text{imp}}(\text{curl})$, $\mathbf{B}_0 \in H_{\text{imp}}(\text{div})$, and we assume that \mathbf{B}_0 is divergence-free. As is well known, this assumption implies that \mathbf{B} is divergence-free for all $t > 0$. Even though there are no derivatives acting on \mathbf{B} in the variational form, we choose $\mathbf{B} \in H_{\text{imp}}(\text{div})$, because $\text{div } \mathbf{B} = 0$ is enforced strongly and, therefore, $\mathbf{B} \in H(\text{div})$.

Remark 3.1. Regarding the existence and uniqueness of the solution to the variational problem, (3.5)–(3.7), we point out that in the case of a perfect conductor, solution results for Lipschitz polyhedra are found in Pauly and Rossi [18] and also in Birman and Solomyak [5, 6]. However, for the dissipative boundary conditions we consider and for Lipschitz polyhedral domains, to our best knowledge there are no results on existence and uniqueness. For solution results on smooth domains (C^1) we refer to the monograph by Petkov [19], where the general case of symmetric hyperbolic systems is considered and existence and uniqueness are derived using semigroup theory. For Lipschitz polyhedral domains it is not straightforward and is difficult to see that the solution is related to a contraction semigroup.

Next, the following proposition shows that for a divergence-free $\mathbf{E}_0 \in H_{\text{imp}}(\text{curl}; t)$, the variational form satisfies the divergence-free condition for \mathbf{E} weakly for all time.

PROPOSITION 3.1. *Let $u = (\mathbf{E}, \mathbf{B}, p)$ satisfy (3.5)–(3.7) and the initial conditions (3.8). If $\mathbf{E}_0 \in H_{\text{imp}}(\text{curl})$ is weakly divergence-free, then for all t and \mathbf{x} , $p(t, \mathbf{x}) = 0$ and, hence,*

$$(\mathbf{E}, \text{grad } q) = 0 \quad \text{for all } q \in H_0^1(\Omega).$$

Proof. In (3.7), take $q \in H_0^1(\Omega)$, then differentiate with respect to t to get

$$(3.9) \quad (p_{tt}, q) = (\mathbf{E}_t, \text{grad } q) \quad \text{for all } q \in H_0^1(\Omega).$$

In the first equation, (3.5), set $\mathbf{F} = \text{grad } q$. Note that the tangential component of $\text{grad } q$ is zero, because $q \in H_0^1(\Omega)$ has a vanishing trace on the boundary of Ω . Thus, the boundary term vanishes and we are left with

$$(\mathbf{E}_t, \text{grad } q) = -(\text{grad } p, \text{grad } q) + (\mathbf{B}, \text{curl } \text{grad } q) - (\mathbf{j}, \text{grad } q).$$

Using integration by parts on the last term yields

$$(\mathbf{j}, \text{grad } q) = \int_{\partial\Omega} (\mathbf{n} \cdot \mathbf{j})q - (\text{div } \mathbf{j}, q) = 0,$$

since \mathbf{j} is divergence-free and q vanishes on the boundaries. Taking this into account, along with (3.9) and the identity $\text{curl } \text{grad} = 0$, rewrite (3.5) as follows:

$$(3.10) \quad (p_{tt}, q) + (\text{grad } p, \text{grad } q) = 0 \quad \text{for all } q \in H_0^1(\Omega).$$

Since $p(0) = 0$ and $p_t(0) = -\operatorname{div} \mathbf{E}(0) = 0$, it is concluded that $p(t, \mathbf{x}) = 0$ for all $t > 0$ and all $\mathbf{x} \in \Omega$, since it is a solution of the homogeneous wave equation, i.e., (3.10). The condition $p_t(0) = -\operatorname{div} \mathbf{E}(0)$ comes from integrating (3.7) by parts and noting that q vanishes on the boundary. Then, from (3.7), the desired result for \mathbf{E} follows. \square

Next, we show an energy estimate.

PROPOSITION 3.2. *Let $u = (\mathbf{E}, \mathbf{B}, p)$ satisfy (3.5)–(3.7) and the initial conditions (3.8). Assume that $\mathbf{j} = \mathbf{0}$ (i.e., no external forces). Then, the following estimate holds for all $T \geq 0$:*

$$\|p(T, \cdot)\|^2 + \|\mathbf{E}(T, \cdot)\|^2 + \|\mathbf{B}(T, \cdot)\|^2 \leq \|\mathbf{E}_0\|^2 + \|\mathbf{B}_0\|^2.$$

Proof. Fix t and take $(q, \mathbf{F}, \mathbf{C}) = (p, \mathbf{E}, \mathbf{B})$. Summing up the three equations (3.5)–(3.7) gives

$$(3.11) \quad \frac{d}{dt} (\|p\|^2 + \|\mathbf{E}\|^2 + \|\mathbf{B}\|^2) = -2(1 + \gamma) \|\mathbf{E}_{\tan}\|_{L^2(\Gamma_i)}^2.$$

This identity holds for any t and the proof is concluded after integrating with respect to time. \square

4. Finite-element discretization.

4.1. Domain partitioning. To devise a discretization of (3.5)–(3.7), we approximate the exterior of the sphere by a polyhedral domain, which is decomposed as a union of simplices (tetrahedrons). The polyhedral domain and its splitting is obtained by mapping a corresponding splitting of a cube to a polyhedron with vertices on the sphere.

We consider a cube $\tilde{\Omega} = (-R/2, R/2)^3$ and we split it into $\frac{R^3}{h^3}$ cubes each with side length h and integer $R > 1$. Here $h = 2^{-J}$ for some $J \geq 2$. From this partition, we remove all cubes that have nonempty intersection with the open cube $\tilde{\omega} = (-1/2, 1/2)^3$. Finally, we split each of the cubes from the lattice into six tetrahedrons and this gives a partitioning of $\tilde{\Omega} \setminus \tilde{\omega}$ into simplices. Note that this partition has the same vertices as the lattice and

$$\overline{\tilde{\Omega} \setminus \tilde{\omega}} = \cup_{K \in \mathcal{T}_h} \overline{K}.$$

From this, we obtain a polyhedron approximating the region between two spheres by mapping a vertex of the lattice whose Cartesian coordinates are \mathbf{x} and whose spherical coordinates are $(|\mathbf{x}|_{\ell_2}, \theta, \phi)$ to the point with spherical coordinates $(|\mathbf{x}|_{\ell_\infty}, \theta, \phi)$. Clearly this maps the interior boundary of $\overline{\tilde{\Omega} \setminus \tilde{\omega}}$ to the unit sphere and maps the outer boundary to a sphere with radius R . An example is shown in Figures 4.1 and 4.2. We note that when $h \rightarrow 0$ the corresponding polyhedron approximates the region between the spheres.

4.2. Finite-element spaces. For the discrete problem, we use standard piecewise linear continuous elements paired with Nédélec [16, 17] finite-element spaces. We introduce the spaces $H_{h,\text{imp}}(\operatorname{curl}) \subset \tilde{H}_{\text{imp}}(\operatorname{curl})$ and $H_{h,\text{imp}}(\operatorname{div}) \subset H_{\text{imp}}(\operatorname{div})$, and the FE solution is denoted by $(\mathbf{E}^h, \mathbf{B}^h, p^h) \in H_{h,\text{imp}}(\operatorname{curl}) \times H_{h,\text{imp}}(\operatorname{div}) \times H_h(\operatorname{grad})$. More precisely, we define

$$\begin{aligned} H_{h,\text{imp}}(\operatorname{div}) &= \{\mathbf{C} \in H_{h,\text{imp}}(\operatorname{div}), \mathbf{C}|_K = \mathbf{a}_K + \beta_K \mathbf{x} \text{ for all } K \in \mathcal{T}_h\}, \\ H_{h,0}(\operatorname{grad}) &= \{q \in H_0^1(\Omega), q|_K \text{ is linear in } \mathbf{x} \text{ for all } K \in \mathcal{T}_h\}. \end{aligned}$$

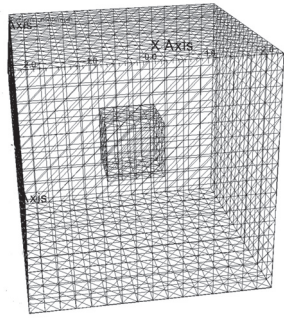


FIG. 4.1. *Cube obstacle.*

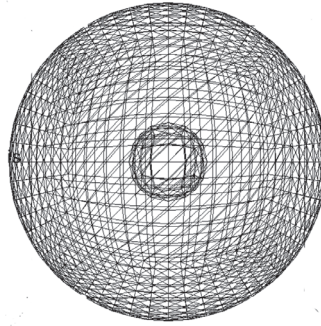


FIG. 4.2. *Sphere obstacle.*

The space $H_{h,\text{imp}}(\text{curl})$ is a properly chosen subspace of $\tilde{H}_{h,\text{imp}}(\text{curl})$, which is orthogonal to the gradients of the *discrete* harmonic forms (but not necessarily to $\text{grad } \mathfrak{h}$). This intermediate space is defined as

$$\tilde{H}_{h,\text{imp}}(\text{curl}) = \{ \mathbf{F} \in \tilde{H}_{\text{imp}}(\text{curl}), \mathbf{F}|_K = \mathbf{a}_K + \mathbf{b}_K \wedge \mathbf{x} \text{ for all } K \in \mathcal{T}_h \}.$$

Next, the discrete harmonic form, \mathfrak{h}^h , is defined as the unique piecewise linear continuous function satisfying

$$\begin{aligned} (\text{grad } \mathfrak{h}^h, \text{grad } q) &= 0 \quad \text{for all } q \in H_{h,0}(\text{grad}), \\ \mathfrak{h}^h &= 1 \quad \text{on } \Gamma_i, \\ \mathfrak{h}^h &= 0 \quad \text{on } \Gamma_o. \end{aligned}$$

Then,

$$H_{h,\text{imp}}(\text{curl}) = \{ \mathbf{F} \in \tilde{H}_{h,\text{imp}}(\text{curl}), (\mathbf{F}, \text{grad } \mathfrak{h}^h) = 0 \}.$$

In the definitions above, $\mathbf{a}_K, \mathbf{b}_K \in \mathbb{R}^3$ are constant vectors for every simplex K in the partition and $\beta_K \in \mathbb{R}$.

Spaces corresponding to the time-dependent problem are analogously defined using the definitions from the previous section. We denote these spaces by $H_{h,\text{imp}}(\text{curl}; t)$, $H_{h,\text{imp}}(\text{div}; t)$, and $H_{h,0}(\text{grad}; t)$, respectively. Note that $\mathbf{v} \in H_{\text{imp}}(\text{curl}; t)$ implies that the tangential components of \mathbf{v} are continuous. The other spaces induce certain compatibility conditions as well. For example, the requirement $\mathbf{B} \in H(\text{div}; t)$ in the definition of the space $H_{h,\text{imp}}(\text{div}; t)$ at the beginning of section 4.2 is equivalent to saying that the *normal* components of the elements from $H_{h,\text{imp}}(\text{div}; t)$ are continuous across element faces. It is also easy to check that $q \in H_{h,0}(\text{grad}; t) \subset H_0^1(\Omega)$ in the definition above implies that q is a continuous function (because it is a piecewise polynomial function, which is in $H_0^1(\Omega)$).

Finally, it is important to note that (3.5)–(3.7) make sense for all $\mathbf{E} \in H(\text{curl})$. As stated above, the piecewise polynomial functions on tetrahedral partitions of Ω are in $H(\text{curl})$ if their tangential components across the faces are continuous. Such functions, however, do not necessarily have continuous normal component across the faces of the tetrahedrons. Thus, the approximation \mathbf{E}^h to \mathbf{E} is not in $H(\text{div})$ even though $\mathbf{E} \in H(\text{div})$.

4.3. Discrete weak form. After constructing the approximating spaces, the discrete problem is constructed by restricting the bilinear form onto the piecewise polynomial spaces. In the following, we set $\mathbf{j} = 0$ because we are interested only in the dependence of the solution on initial conditions. Denoting

$$H_h = H_{h,\text{imp}}(\text{curl}) \times H_{h,\text{imp}}(\text{div}) \times H_{h,0}(\text{grad})$$

and restricting (3.5)–(3.7) to H_h leads to the following approximate variational problem: Find $(\mathbf{E}^h, \mathbf{B}^h, p^h) \in H_h$ such that for all $(\mathbf{F}^h, \mathbf{C}^h, q^h) \in H_h$

$$(4.1) \quad (\mathbf{E}_t^h, \mathbf{F}^h) = -(\text{grad } p^h, \mathbf{F}^h) + (\mathbf{B}^h, \text{curl } \mathbf{F}^h) - (1 + \gamma) \int_{\Gamma_i} \langle \mathbf{n} \wedge \mathbf{E}^h, \mathbf{n} \wedge \mathbf{F}^h \rangle,$$

$$(4.2) \quad (\mathbf{B}_t^h, \mathbf{C}^h) = -(\text{curl } \mathbf{E}^h, \mathbf{C}^h),$$

$$(4.3) \quad (p_t^h, q^h) = (\mathbf{E}^h, \text{grad } q^h).$$

In the following, the superscript h is omitted, since the considerations in the rest of the paper are focused on the discrete problem in H_h . We also interchangeably use \mathbf{u} and $(\mathbf{E}, \mathbf{B}, p)^T$ and, similarly, \mathbf{w} and $(\mathbf{F}, \mathbf{C}, q)^T$.

An operator is introduced such that $\mathcal{A} : H_h \mapsto H_h$ via the bilinear forms in (4.1)–(4.3). For $\mathbf{u} = (\mathbf{E}, \mathbf{B}, p)^T \in H_h$ and $\mathbf{w} = (\mathbf{F}, \mathbf{C}, q)^T \in H_h$, set

$$(\mathcal{A}\mathbf{u}, \mathbf{w}) = -(\mathbf{E}, \text{grad } q) + (\text{grad } p, \mathbf{F}) - (\mathbf{B}, \text{curl } \mathbf{F}) + (\text{curl } \mathbf{E}, \mathbf{C}).$$

Corresponding to the boundary term, we also have the operator associated with the impedance boundary condition,

$$(\mathcal{Z}\mathbf{u}, \mathbf{w}) = (1 + \gamma) \int_{\Gamma_i} \langle \mathbf{n} \wedge \mathbf{E}, \mathbf{n} \wedge \mathbf{F} \rangle.$$

Since we are now on a finite-dimensional space, we write the semidiscrete problem (discretized in space and continuous in time) as a constant coefficient linear system of ODEs, i.e.,

$$(4.4) \quad \dot{\mathbf{u}} = -(\mathcal{A} + \mathcal{Z})\mathbf{u}.$$

From the definitions of \mathcal{A} and \mathcal{Z} it is obvious that \mathcal{A} is skew symmetric and \mathcal{Z} is symmetric and positive semidefinite.

5. Matrix representation and time discretization. We now show that the assembly of system (4.4) can be constructed using only mass (Gramm) matrices formed with the bases in $H_{h,\text{imp}}(\text{curl})$, $H_{h,\text{imp}}(\text{div})$, and $H_{h,0}(\text{grad})$ spaces and incidence matrices, whose entries encode the relationships “vertex incident to an edge,” “edge incident to a face,” etc. The aim of this section is to provide some insight into the implementation of such finite-element schemes and also to set the stage for presenting the Crank–Nicolson discretization in time.

5.1. Matrix representation. We start with a description of the standard (canonical) bases in $H_{h,0}(\text{grad})$, $H_{h,\text{imp}}(\text{div})$, and $H_{h,\text{imp}}(\text{curl})$, respectively. By boundary vertices, edges, and faces we mean vertices, edges, and faces lying on the boundary, $\partial\Omega$. For an edge, this means that both its end vertices are on the boundary and for a face it means that all three of its vertices are on the boundary. The remaining vertices (edges, faces) are designated as interior vertices (edges, faces). We note that by

a standard convention, it is assumed that for the triangulation in hand the directions of vectors tangential to edges and normal to faces are fixed once and for all. It is easy and straightforward to check that a change in these directions does not change the considerations that follow.

We then have the following sets of degrees of freedom (DoFs):

- DoFs corresponding to the set of interior vertices $\{\mathbf{x}_i\}_{i=1}^{n_h}$: A functional (also denoted by \mathbf{x}_i) is associated with an interior vertex \mathbf{x}_i as $\mathbf{x}_i(q) = q(\mathbf{x}_i)$ for a sufficiently smooth function, q .
- DoFs corresponding to the set of all interior edges and all edges on Γ_i : For a sufficiently smooth vector-valued function, \mathbf{v} , and an edge, $e \in \mathcal{E}$, the associated functional is $e(\mathbf{v}) = \frac{1}{|e|} \int_e \mathbf{v} \cdot \boldsymbol{\tau}_e$, where $\boldsymbol{\tau}_e$ is the unit vector tangential to the edge. The direction of the tangent vector, $\boldsymbol{\tau}_e$, is assumed to be fixed.
- DoFs corresponding to the set of interior faces, \mathcal{F} : For a sufficiently smooth vector-valued function, \mathbf{v} , and a face $f \in \mathcal{F}$, the associated functional is $f(\mathbf{v}) = \frac{1}{|f|} \int_f \mathbf{v} \cdot \mathbf{n}_f$, where \mathbf{n}_f is the unit vector normal to the face.

As bases for the spaces $H_{h,0}(\text{grad})$, $H_{h,\text{imp}}(\text{curl})$, and $H_{h,\text{imp}}(\text{div})$ we take the piecewise polynomial functions, which are dual to the functionals given above. For the space $H_{h,0}(\text{grad})$, we denote these functions by $\{\varphi_j\}_{j=1}^{n_h}$. They are piecewise linear, are continuous, and satisfy $\mathbf{x}_k(\varphi_j) = \delta_{kj}$, where δ_{kj} is the Kronecker delta.

The bases for the other two spaces $H_{h,\text{imp}}(\text{curl})$ and $H_{h,\text{imp}}(\text{div})$ are then given in terms of the basis for $H_{h,0}(\text{grad})$. For an edge $e \in \mathcal{E}$ with vertices $(\mathbf{x}_i, \mathbf{x}_j)$ and a face $f \in \mathcal{F}$ with vertices $(\mathbf{x}_i, \mathbf{x}_j, \mathbf{x}_k)$,

$$\begin{aligned} \boldsymbol{\psi}_e &= |e|(\varphi_i \text{grad } \varphi_j - \varphi_j \text{grad } \varphi_i), \\ \boldsymbol{\xi}_f &= |f|(\varphi_i(\text{grad } \varphi_j \wedge \text{grad } \varphi_k) + \varphi_j(\text{grad } \varphi_k \wedge \text{grad } \varphi_i) + \varphi_k(\text{grad } \varphi_i \wedge \text{grad } \varphi_j)). \end{aligned}$$

Here, $\boldsymbol{\tau}_e = (\mathbf{x}_j - \mathbf{x}_i)/|\mathbf{x}_i - \mathbf{x}_j|$ and the ordering of $(\mathbf{x}_i, \mathbf{x}_j, \mathbf{x}_k)$ in a positive direction is determined by the right-hand rule and the normal vector \mathbf{n}_f . We then have the following canonical representations of functions in $H_{h,\text{imp}}(\text{curl})$, $H_{h,\text{imp}}(\text{div})$, and $H_{h,0}(\text{grad})$:

$$\begin{aligned} \mathbf{v} \in H_{h,\text{imp}}(\text{curl}), \quad \mathbf{v} &= \sum_{e \in \mathcal{E}} e(\mathbf{v}) \boldsymbol{\psi}_e(\mathbf{x}); & \mathbf{v} \in H_{h,\text{imp}}(\text{div}), \quad \mathbf{v} &= \sum_{f \in \mathcal{F}} f(\mathbf{v}) \boldsymbol{\xi}_f(\mathbf{x}); \\ q \in H_{h,0}(\text{grad}), \quad q &= \sum_{i=1}^{n_h} \mathbf{x}_i(q) \varphi_i(\mathbf{x}). \end{aligned}$$

For functions that also depend on time, i.e., for the elements of $H_{h,\text{imp}}(\text{curl}; t)$, $H_{h,\text{imp}}(\text{div}; t)$, and $H_{h,0}(\text{grad}; t)$, we have similar representations with coefficients depending on time as well.

Remark 5.1. In the rest of the paper, the same notation is used for the functions from H_h and their vector representations in the bases given above. This is done in order to simplify the notation.

The entries of the mass (Gramm) matrices for each of the piecewise polynomial spaces are then

$$(\mathcal{M}_e)_{ee'} = (\boldsymbol{\psi}_e, \boldsymbol{\psi}_{e'}), \quad (\mathcal{M}_f)_{ff'} = (\boldsymbol{\xi}_f, \boldsymbol{\xi}_{f'}), \quad (\mathcal{M}_v)_{ij} = (\varphi_i, \varphi_j).$$

Next, the following matrix representations of the operators defined in the previous section are introduced:

$$\mathcal{G}_{ej} = (\text{grad } \varphi_j, \boldsymbol{\psi}_e), \quad \mathcal{K}_{fe} = (\text{curl } \boldsymbol{\psi}_e, \boldsymbol{\xi}_f).$$

Downloaded 11/05/13 to 130.64.11.153. Redistribution subject to SIAM license or copyright; see http://www.siam.org/journals/ojsa.php

The matrix form of (4.4) is now rewritten as follows:

$$(5.1) \quad \begin{pmatrix} \mathcal{M}_e & & \\ & \mathcal{M}_f & \\ & & \mathcal{M}_v \end{pmatrix} \begin{pmatrix} \dot{\mathbf{E}} \\ \dot{\mathbf{B}} \\ \dot{p} \end{pmatrix} = \left[\begin{pmatrix} & \mathcal{K}^T \mathcal{M}_f & -\mathcal{M}_e \mathcal{G} \\ -\mathcal{M}_f \mathcal{K} & & \\ \mathcal{G}^T \mathcal{M}_e & & \end{pmatrix} - \mathcal{Z} \right] \begin{pmatrix} \mathbf{E} \\ \mathbf{B} \\ p \end{pmatrix}.$$

5.2. Time discretization. To discretize system (5.1) in time, a Crank–Nicolson scheme is used. We look at a time interval, $t \in [0, T]$, and approximate the solution at $t = k\tau$, $k = 1, \dots, \frac{T}{\tau}$, with τ a given time step. Let $\mathbf{u}_k = (\mathbf{E}_k, \mathbf{B}_k, p_k)^T$ be the discrete approximation at the current time $t = k\tau$, and let $\mathbf{u}_{k-1} = (\mathbf{E}_{k-1}, \mathbf{B}_{k-1}, p_{k-1})^T$ be the approximation at the previous time $t = (k-1)\tau$. Then, the Crank–Nicolson formulation of (5.1) is

$$\frac{1}{\tau} \mathcal{M}(\mathbf{u}_k - \mathbf{u}_{k-1}) = -\frac{1}{2}(\mathcal{A} + \mathcal{Z})(\mathbf{u}_k + \mathbf{u}_{k-1}), \quad \text{where } \mathcal{M} = \begin{pmatrix} \mathcal{M}_e & & \\ & \mathcal{M}_f & \\ & & \mathcal{M}_v \end{pmatrix}.$$

Rearranging the terms, we get the following linear system for the approximate solution at time step $k\tau$ in terms of the solution at time $(k-1)\tau$:

$$(5.2) \quad \left(\frac{1}{\tau} \mathcal{M} + \frac{1}{2}(\mathcal{A} + \mathcal{Z}) \right) \mathbf{u}_k = \left(\frac{1}{\tau} \mathcal{M} - \frac{1}{2}(\mathcal{A} + \mathcal{Z}) \right) \mathbf{u}_{k-1}.$$

Next, we show that if the initial condition is weakly divergence-free, as in the continuous case, we have that p_k will remain zero for all time and, thus, \mathbf{E}_k is weakly divergence-free for all k . This is the discrete analogue of Proposition 3.1.

LEMMA 5.1. *Assume that $(\mathbf{E}_0, \text{grad } q) = 0$ for all $q \in H_{h,0}(\text{grad})$. For the Crank–Nicolson scheme described in (5.2), $p_k = 0$ for all k and $(\mathbf{E}_k, \text{grad } q) = 0$ for all $q \in H_{h,0}(\text{grad})$ and all k .*

Proof. Start with $p_0 = 0$ and \mathbf{E}_0 being weakly divergence-free. It is shown that

$$\text{if } p_k = 0 \quad \text{and} \quad \mathcal{G}^T \mathcal{M}_e \mathbf{E}_k = 0, \quad \text{then } p_{k+1} = 0 \quad \text{and} \quad \mathcal{G}^T \mathcal{M}_e \mathbf{E}_{k+1} = 0.$$

This is the matrix representation of the assumptions and claims in the lemma. Setting $\alpha = 2/\tau$ and using the defining relations for the Crank–Nicolson time discretization, (5.1) and (5.2), the following linear system for \mathbf{E}_{k+1} , \mathbf{B}_{k+1} , and p_{k+1} is obtained:

$$(5.3) \quad \alpha \mathcal{M}_e \mathbf{E}_{k+1} - \mathcal{K}^T \mathcal{M}_f \mathbf{B}_{k+1} + \mathcal{M}_e \mathcal{G} p_{k+1} + \tilde{\mathcal{Z}} \mathbf{E}_{k+1} = \alpha \mathcal{M}_e \mathbf{E}_k + \mathcal{K}^T \mathcal{M}_f \mathbf{B}_k - \tilde{\mathcal{Z}} \mathbf{E}_k,$$

$$(5.4) \quad \mathcal{M}_f \mathcal{K} \mathbf{E}_{k+1} + \alpha \mathcal{M}_f \mathbf{B}_{k+1} = -\mathcal{M}_f \mathcal{K} \mathbf{E}_k + \alpha \mathcal{M}_f \mathbf{B}_k,$$

$$(5.5) \quad -\mathcal{G}^T \mathcal{M}_e \mathbf{E}_{k+1} + \alpha \mathcal{M}_v p_{k+1} = 0.$$

Here, $\tilde{\mathcal{Z}}$ indicates the reduced matrix of \mathcal{Z} applied to just the edge DoF, \mathbf{E} . Multiplying (5.3) from the left by \mathcal{G}^T yields

$$\begin{aligned} & \alpha \mathcal{G}^T \mathcal{M}_e \mathbf{E}_{k+1} - \mathcal{G}^T \mathcal{K}^T \mathcal{M}_f \mathbf{B}_{k+1} + \mathcal{G}^T \mathcal{M}_e \mathcal{G} p_{k+1} + \mathcal{G}^T \tilde{\mathcal{Z}} \mathbf{E}_{k+1} \\ & = \alpha \mathcal{G}^T \mathcal{M}_e \mathbf{E}_k + \mathcal{G}^T \mathcal{K}^T \mathcal{M}_f \mathbf{B}_k - \mathcal{G}^T \tilde{\mathcal{Z}} \mathbf{E}_k. \end{aligned}$$

Next, note that $\mathcal{K} \mathcal{G} = 0$ (or equivalently $\mathcal{G}^T \mathcal{K}^T = 0$), since the curl of a gradient is zero. Also, since any $q \in H_{h,0}(\text{grad}) \subset H_0^1(\Omega)$ is zero on Γ_i and Γ_o and the tangential component of its gradient is zero on the boundary edges, then $\tilde{\mathcal{Z}} \mathcal{G} = 0$ (or equivalently $\mathcal{G}^T \tilde{\mathcal{Z}} = 0$, since $\tilde{\mathcal{Z}}$ is symmetric). Thus, (5.3) simplifies to

$$\alpha \mathcal{G}^T \mathcal{M}_e \mathbf{E}_{k+1} + \mathcal{G}^T \mathcal{M}_e \mathcal{G} p_{k+1} = 0.$$

Adding this to α times (5.5) then gives

$$(5.6) \quad (\mathcal{G}^T \mathcal{M}_e \mathcal{G} + \alpha^2 \mathcal{M}_v) p_{k+1} = 0.$$

The above relation is the matrix representation of the variational problem,

$$(\text{grad } p_{k+1}, \text{grad } q) + \alpha^2 (p_{k+1}, q) = 0 \quad \text{for all } q \in H_{h,0}(\text{grad}),$$

and taking $q = p_{k+1}$ then gives that $p_{k+1} = 0$. Finally, from this fact and using (5.5), it is immediately shown that $\mathcal{G}^T \mathcal{M}_e \mathbf{E}_{k+1} = 0$, concluding the proof. \square

Thus, using the Crank–Nicolson scheme and appropriate initial conditions, one can guarantee that the discrete approximation to the electric field will be weakly divergence-free for all time.

5.3. Solution of the discrete linear systems. To solve the system, we look at the matrix corresponding to $\frac{1}{\tau} \mathcal{M} + \frac{1}{2} (\mathcal{A} + \mathcal{Z})$, which is on the left side of (5.2). We have to solve the system with this matrix at every time step. Using the incidence matrices as in (4.4), this operator is written as

$$\frac{1}{\tau} \mathcal{M} + \frac{1}{2} (\mathcal{A} + \mathcal{Z}) = \frac{1}{2} \begin{pmatrix} \frac{2}{\tau} \mathcal{M}_e & -\mathcal{K}^T \mathcal{M}_f & \mathcal{M}_e \mathcal{G} \\ \mathcal{M}_f \mathcal{K} & \frac{2}{\tau} \mathcal{M}_f & \\ -\mathcal{G}^T \mathcal{M}_e & & \frac{2}{\tau} \mathcal{M}_v \end{pmatrix} + \frac{1}{2} \mathcal{Z}.$$

Since the mass matrices $\mathcal{M}_e, \mathcal{M}_f, \mathcal{M}_v$ are all symmetric positive definite and \mathcal{Z} is symmetric positive semidefinite and only contributes to the edge-edge diagonal block of the system, the entire operator can be made symmetric by a simple permutation. Multiplying on the left by $J = \begin{pmatrix} I & & \\ & -I & \\ & & -I \end{pmatrix}$ will yield the operator

$$J \left(\frac{1}{\tau} \mathcal{M} + \frac{1}{2} (\mathcal{A} + \mathcal{Z}) \right) = \begin{pmatrix} \frac{1}{\tau} \mathcal{M}_e & -\frac{1}{2} \mathcal{K}^T \mathcal{M}_f & +\frac{1}{2} \mathcal{M}_e \mathcal{G} \\ -\frac{1}{2} \mathcal{M}_f \mathcal{K} & -\frac{1}{\tau} \mathcal{M}_f & \\ \frac{1}{2} \mathcal{G}^T \mathcal{M}_e & & -\frac{1}{\tau} \mathcal{M}_v \end{pmatrix} + \frac{1}{2} \mathcal{Z},$$

which is now symmetric. Therefore, the final system to solve is

$$(5.7) \quad \mathcal{J} \left(\frac{1}{\tau} \mathcal{M} + \frac{1}{2} (\mathcal{A} + \mathcal{Z}) \right) \mathbf{u}_n = \mathcal{J} \left(\frac{1}{\tau} \mathcal{M} - \frac{1}{2} (\mathcal{A} + \mathcal{Z}) \right) \mathbf{u}_{n-1},$$

and a standard iterative solver such as MINRES can be applied. This is used in the test problems below.

6. Numerical results. Here, we perform some numerical tests by solving system (5.7) using the Crank–Nicolson time discretization described in the previous section. To test for decay in the energy of the solution, we start with initial conditions and boundary conditions of the form described in [10]. We take as the domain the area between a polyhedral approximation of the sphere of radius 1 and a polyhedral approximation of a sphere of radius 4. The inner sphere represents the impedance boundary and the outer sphere is considered far enough away (and it is for the solutions we approximate) that a Dirichlet-like perfect conductor boundary condition on the outer sphere is used. In other words, we prescribe $\mathbf{E} \wedge \mathbf{n}, \mathbf{B} \cdot \mathbf{n}$, and $p = 0$ on the outer sphere. The exact solution (taken from [10, Theorem 3.2]) is given as follows:

Downloaded 11/05/13 to 130.64.11.153. Redistribution subject to SIAM license or copyright; see http://www.siam.org/journals/ojsa.php

$$(6.1) \quad \mathbf{E}_* = \frac{e^{r(|\mathbf{x}|+t)}}{|\mathbf{x}|^2} \begin{pmatrix} r^2 - \frac{r}{|\mathbf{x}|} \\ 0 \\ z \\ -y \end{pmatrix},$$

$$(6.2) \quad \mathbf{B}_* = e^{r(|\mathbf{x}|+t)} \left[\frac{1}{|\mathbf{x}|^3} \left(r^2 - \frac{3r}{|\mathbf{x}|} + \frac{3}{|\mathbf{x}|^2} \right) \begin{pmatrix} z^2 + y^2 \\ -xy \\ -xz \end{pmatrix} + \begin{pmatrix} \frac{2r}{|\mathbf{x}|} - \frac{2}{|\mathbf{x}|^2} \\ 0 \\ 0 \end{pmatrix} \right].$$

Different values of γ yield different values of r in solutions (6.1)–(6.2). Following [10], we have that $(\mathbf{E}_*, \mathbf{B}_*, 0)$ solves Maxwell's system with an impedance boundary condition on Γ_i and

$$r = 1/2 \left(1 - \sqrt{1 + 4/\gamma} \right).$$

For the tests below, we take $\gamma = 0.05$ ($r = -4$).

For the annular domain that we consider, a basis in the one-dimensional space of harmonic forms is of the form $\text{grad } \mathfrak{h} = \mathbf{x}/|\mathbf{x}|^3$. Direct computation shows that $\langle \mathbf{E}_*, \text{grad } \mathfrak{h} \rangle = 0$, and this identity holds pointwise and for all t . Thus, the ADS that we are trying to approximate is orthogonal to the harmonic forms in this particular example.

6.1. Approximation of the initial conditions. Since the solutions given above are not in the finite-dimensional spaces considered, we take an initial condition \mathbf{E}_0 , which is based on the piecewise polynomial interpolant of the exponentially decaying solution given in (6.1) at $t = 0$. In other words, we set

$$(6.3) \quad \tilde{\mathbf{E}}_0 = \sum_{e \in \mathcal{E}} e(\mathbf{E}_*(0, \mathbf{x})) \psi_e(\mathbf{x}).$$

Remark 6.1. We noted earlier that the ADS given by (6.1) is orthogonal to all harmonic forms. However, this is not so for the discrete approximation in (6.3). We perform an orthogonalization step and take initial conditions that are orthogonal to the *discrete* harmonic forms in order to approximate the ADS and the energy decay more accurately.

We further correct $\tilde{\mathbf{E}}_0$ to get an initial guess that is orthogonal to the gradients as well as the gradients of the discrete harmonic form, $\text{grad } \mathfrak{h}^h$. This is done in a standard fashion by projecting out these gradients. First, we find $s \in H_{0,h}(\text{grad})$ such that for all $q \in H_{0,h}(\text{grad})$, we have

$$(\text{grad } s, \text{grad } q) = (\tilde{\mathbf{E}}_0, \text{grad } q), \quad \mathbf{E}_0 = \tilde{\mathbf{E}}_{0,h} - \text{grad } s - \frac{(\tilde{\mathbf{E}}_{0,h}, \text{grad } \mathfrak{h}^h)}{\|\text{grad } \mathfrak{h}^h\|^2} \text{grad } \mathfrak{h}^h.$$

As a result, \mathbf{E}_0 is orthogonal to the gradients of functions in $H_{0,h}(\text{grad})$ and also to the gradient of the discrete harmonic form. We note that this orthogonalization requires two solutions of Laplace equation. It is straightforward to see that if the initial guess satisfies such condition, then the solution \mathbf{E} satisfies this condition for all times. Finally, \mathbf{B}_0 is computed as $\mathbf{B}_0 = \frac{1}{r} \mathcal{K} \mathbf{E}_0$.

6.2. Numerical results. We test the approximation to the ADS on a grid with 728 ($h = 1/8$), 4,886 ($h = 1/16$), 35,594 ($h = 1/32$), and 271,250 ($h = 1/64$) nodes on the domain. The computational domain is shown in Figure 4.2. We run a MINRES solver on the Crank–Nicolson system that is symmetrized, (5.7), for 20 time steps using a step size $\tau = 0.1$.

The results are shown in Tables 6.1–6.4, where we display the $\|\mathbf{E}\|_{L_2(\Omega)}$ and $\|\mathbf{B}\|_{L_2(\Omega)}$ norms. The total energy of this system is given by $\|\mathbf{E}\|_{L_2(\Omega)}^2 + \|\mathbf{B}\|_{L_2(\Omega)}^2$.

Tables 6.1–6.4 show that over time the L_2 norms of the electric and magnetic fields decay. For each mesh size, it appears that the energy reaches some steady-state value, where it does not decay anymore. Figure 6.1 shows that this final energy value (at time step 20), $\|\mathbf{E}\|_{L_2(\Omega)}^2 + \|\mathbf{B}\|_{L_2(\Omega)}^2$, decreases as h^2 , when $h \rightarrow 0$. Thus, as the

TABLE 6.1
Sphere obstacle. $\gamma = 0.05$. $h = 1/8$.

Step	$\ \mathbf{E}\ _{L_2(\Omega)}$	$\ \mathbf{B}\ _{L_2(\Omega)}$
0	0.906	0.559
1	0.830	0.334
2	0.723	0.155
3	0.614	0.116
4	0.526	0.172
5	0.450	0.242
6	0.380	0.304
7	0.316	0.349
8	0.262	0.379
9	0.233	0.389
10	0.234	0.384
11	0.248	0.373
12	0.266	0.358
13	0.284	0.339
14	0.292	0.322
15	0.288	0.312
16	0.276	0.307
17	0.262	0.303
18	0.251	0.299
19	0.248	0.293
20	0.246	0.287

TABLE 6.2
Sphere obstacle. $\gamma = 0.05$. $h = 1/16$.

Step	$\ \mathbf{E}\ _{L_2(\Omega)}$	$\ \mathbf{B}\ _{L_2(\Omega)}$
0	0.553	0.426
1	0.451	0.266
2	0.349	0.153
3	0.267	0.093
4	0.200	0.086
5	0.147	0.103
6	0.117	0.103
7	0.107	0.099
8	0.104	0.097
9	0.095	0.101
10	0.088	0.103
11	0.085	0.104
12	0.084	0.104
13	0.085	0.102
14	0.086	0.100
15	0.086	0.099
16	0.086	0.099
17	0.085	0.099
18	0.086	0.097
19	0.085	0.095
20	0.085	0.095

TABLE 6.3
Sphere obstacle. $\gamma = 0.05$. $h = 1/32$.

Step	$\ \mathbf{E}\ _{L_2(\Omega)}$	$\ \mathbf{B}\ _{L_2(\Omega)}$
0	0.425	0.405
1	0.308	0.262
2	0.214	0.163
3	0.148	0.102
4	0.103	0.061
5	0.074	0.044
6	0.057	0.039
7	0.046	0.037
8	0.040	0.035
9	0.035	0.034
10	0.033	0.034
11	0.032	0.034
12	0.031	0.035
13	0.031	0.034
14	0.031	0.034
15	0.031	0.034
16	0.031	0.034
17	0.031	0.033
18	0.031	0.033
19	0.030	0.033
20	0.031	0.032

TABLE 6.4
Sphere obstacle. $\gamma = 0.05$. $h = 1/64$.

Step	$\ \mathbf{E}\ _{L_2(\Omega)}$	$\ \mathbf{B}\ _{L_2(\Omega)}$
0	0.383	0.401
1	0.261	0.264
2	0.176	0.172
3	0.120	0.113
4	0.081	0.075
5	0.056	0.051
6	0.039	0.034
7	0.028	0.025
8	0.021	0.020
9	0.017	0.017
10	0.015	0.015
11	0.014	0.015
12	0.013	0.015
13	0.012	0.015
14	0.013	0.014
15	0.013	0.014
16	0.013	0.014
17	0.012	0.015
18	0.013	0.014
19	0.013	0.014
20	0.013	0.014

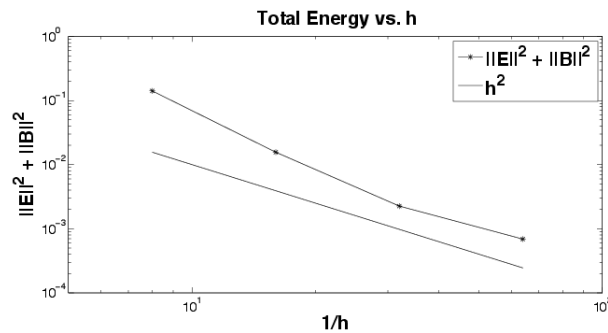


FIG. 6.1. Plot of total energy ($\|E\|_{L_2(\Omega)}^2 + \|B\|_{L_2(\Omega)}^2$) versus mesh size after 20 time steps. The x -axis shows $1/h$.

polyhedron domain more closely represents the spherical domain, as in [10], the total energy should decay to zero as expected over time.

7. Concluding remarks. We have shown that using appropriate finite-element spaces, one can approximate the asymptotically disappearing solutions to Maxwell's equations on the exterior of a spherical obstacle. We also have shown that the Crank–Nicolson time discretization keeps the electric and magnetic fields divergence-free (the electric field weakly and the magnetic field strongly). The next step is to apply the methods to more general domains and answer the question of whether ADS exist for obstacles with more complicated geometry. In relation to considering less regular obstacles, there are many open problems for the analysis of systems with dissipative boundary conditions. The computational techniques that we have introduced here easily generalize to cases of variable, matrix valued permittivity and permeability $\varepsilon(x)$ and $\mu(x)$, as well as to more general hyperbolic systems for which the ADS phenomenon occurs.

Acknowledgments. We are grateful to anonymous referees, who provided many valuable remarks and helped us improve the exposition.

REFERENCES

- [1] D. N. ARNOLD, R. S. FALK, AND R. WINTHER, *Finite element exterior calculus, homological techniques, and applications*, Acta Numer., 15 (2006), pp. 1–155.
- [2] D. N. ARNOLD, R. S. FALK, AND J. GOPALAKRISHNAN, *Mixed Finite Element Approximation of the Vector Laplacian with Dirichlet Boundary Conditions*, arXiv:1109.3668, 2011.
- [3] D. N. ARNOLD, R. S. FALK, AND J. GOPALAKRISHNAN, *Finite element exterior calculus: From Hodge theory to numerical stability*, Bull. Amer. Math. Soc. (N.S.), 47 (2010), pp. 281–354.
- [4] D. N. ARNOLD, *On mixed formulations of Maxwell's equations*, private communication, 2011.
- [5] M. S. BIRMAN AND M. Z. SOLOMYAK, *The Maxwell operator in domains with a nonsmooth boundary*, Sibirsk. Mat. Zh., 28 (1987), pp. i, 23–36.
- [6] M. S. BIRMAN AND M. Z. SOLOMYAK, *The selfadjoint Maxwell operator in arbitrary domains*, Algebra i Analiz, 1 (1989), pp. 96–110.
- [7] A. BOSSAVIT, *Whitney forms: A class of finite elements for three-dimensional computations in electromagnetism*, Phys. Sci. Measurement Instrumentation Management Education Rev. IEE Proc. A, 135 (1988), pp. 493–500.
- [8] F. BREZZI, *On the existence, uniqueness and approximation of saddle-point problems arising from Lagrangian multipliers*, Rev. Française Automat. Informat. Rec. Opér. Sér. Rouge, 8 (1974), pp. 129–151.
- [9] F. BREZZI AND M. FORTIN, *Mixed and Hybrid Finite Element Methods*, Springer Ser. in Comput. Math. 15, Springer-Verlag, New York, 1991.

- [10] F. COLOMBINI, V. PETKOV, AND J. RAUCH, *Incoming and disappearing solutions for Maxwell's equations*, Proc. Amer. Math. Soc., 139 (2011), pp. 2163–2173.
- [11] F. COLOMBINI, V. PETKOV, AND J. RAUCH, *Scattering Problems for Nonelliptic Systems with Dissipative Boundary Conditions*, Preprint, arXiv:1303.3743, 2013.
- [12] V. GEORGIEV, *Disappearing solutions for dissipative hyperbolic systems of constant multiplicity*, Hokkaido Math. J., 15 (1986), pp. 357–385.
- [13] R. HIPTMAIR, *Finite elements in computational electromagnetism*, Acta Numer., 11 (2002), pp. 237–339.
- [14] W. MCLEAN, *Strongly Elliptic Systems and Boundary Integral Equations*, Cambridge University Press, Cambridge, UK, 2000.
- [15] P. MONK, *Finite Element Methods for Maxwell's Equations*, Numer. Math. Sci. Comput., Oxford University Press, New York, 2003.
- [16] J.-C. NÉDÉLEC, *Mixed finite elements in \mathbf{R}^3* , Numer. Math., 35 (1980), pp. 315–341.
- [17] J.-C. NÉDÉLEC, *A new family of mixed finite elements in \mathbf{R}^3* , Numer. Math., 50 (1986), pp. 57–81.
- [18] D. PAULY AND T. ROSSI, *Theoretical considerations on the computation of generalized time-periodic waves*, Adv. Math. Sci. Appl., 21 (2011), pp. 105–131.
- [19] V. PETKOV, *Scattering Theory for Hyperbolic Operators*, Stud. Math. Appl. 21, North-Holland, Amsterdam, 1989.
- [20] V. PETKOV, *Scattering problems for symmetric systems with dissipative boundary conditions*, in Studies on Phase Space Analysis and Applications to PDEs, Progr. Nonlinear Differential Equations Appl. 84, Birkhäuser, Boston, 2013.
- [21] P.-A. RAVIART AND J. M. THOMAS, *A mixed finite element method for 2nd order elliptic problems*, in Mathematical Aspects of Finite Element Methods, Lecture Notes in Math., 606, Springer, Berlin, 1977, pp. 292–315.